

THE STREAMER CHAMBER

B. A. DOLGOSHEIN, B. I. LUCHKOV, and B. U. RODIONOV

P. N. Lebedev Physics Institute, Academy of Sciences, U.S.S.R.

Submitted to JETP editor December 10, 1963

J. Exptl. Theoret. Phys. (U.S.S.R.) 46, 1953-1959 (June, 1964)

A new type of gas discharge track chamber is described which efficiently records charged particles irrespective of their direction of motion within the chamber. The mechanism of formation of the particle tracks is discussed. Characteristics of the chamber and the results of investigation of various gas fillings are presented.

THE purpose of this article is to describe in detail the construction and mechanism of operation of a streamer¹⁾ chamber^[1]. The chamber is named by analogy with other track-detecting chambers (bubble chamber, cloud chamber, spark chamber), so that the designation reflects the mechanism of formation of the particle tracks recorded in the chamber. In a streamer chamber, in contrast to a spark chamber, the indication of the place of passage of a particle is not a spark channel but a streamer, or more accurately a whole group of streamers located near the particle path.

Stimulation for the development of the streamer chamber was provided by the unsatisfactory operation of the commonly used multilayer spark or discharge chamber with an interelectrode spacing of the order of a few millimeters^[2,3]. Such chambers, while possessing a number of attractive features (short resolving time and dead time, simplicity of design, and stability of operation), also have important deficiencies: anisotropy in the degree of localization of tracks of particles which have passed at different angles φ to the direction of the electric field E ; indistinguishability of particles originating in the gas and in the chamber electrodes; dependence of the counting efficiency for many particles ("shower" efficiency^[2]) on the number of particles n , and its sharp decrease for $n > 2$ ^[4]; and, finally, practically complete absence of information on the ionizing ability of the particles counted. These deficiencies distinguish multilayer spark and discharge chambers from the true track-detecting chambers (bubble chamber, cloud chamber), which record the trajectories of all particles which have passed during the

resolving time, regardless of their direction of motion, place of origin, and number.

Spark and discharge chambers consisting of one large interelectrode gap (of the order of centimeters or tens of centimeters) do not have some of the deficiencies enumerated^[2,5-7]. In such a chamber the spark follows the particle path with great accuracy^[8], and in a chamber placed in a magnetic field transverse to the electric field E , curved sparks are observed^[9]. The "shower" efficiency of the chamber is $\sim 100\%$ and does not depend on the number of particles in the shower up to $n \approx 50$ ^[10]. Observation through a transparent electrode of particle tracks crossing the chamber at large angles ($60^\circ \lesssim \varphi \lesssim 90^\circ$, the "projection" spark chamber regime^[6]) permits study of complex cases of particle interaction and decay in the chamber gas and highly accurate determination of the curvature of trajectories in a magnetic field parallel to E ^[5]. In the projection discharge chamber the tracks of particles with different ionizing ability are distinguished by their brightness and density^[11]. However, like the multilayer chamber, a spark chamber with one large gap possesses anisotropy of particle localization and does not give a spatial picture of any event occurring in the chamber.

The microwave chamber^[12] and the light chamber^[13] are track-following gas-discharge detectors which record trajectories in space independently of the particle direction, but they have not received wide practical application: the first because of the impossibility of building a chamber of large size and at the same time good spatial resolution, and the second because of the limited brightness of the tracks, as a result of which only tracks of strongly ionizing particles (α -particles from radioactive sources) are observed in the chamber.

¹⁾Mikhaïlov, Roñishvili, and Chikovani^[1] use the designation "track spark chamber."

The streamer chamber possesses all the advantages of a spark chamber (rapid action, simplicity of construction and of auxiliary high voltage techniques, possibility of preparing chambers of large dimensions, etc) and at the same time records with good resolution the spatial picture of any event occurring in the chamber volume.

EXPERIMENTAL APPARATUS

Two chambers were used of the same design, differing only in size. The chambers were built of plastic 50 mm thick and consisted of rectangular frames, to the ends of which electrodes were fastened by pneumatic pressure. The exterior dimensions of the chambers were $70 \times 50 \times 10$ cm and $60 \times 50 \times 25$ cm, and the interelectrode spacing d was 10 and 25 cm. A detailed description of the chamber design, the pneumatic clamping of the electrodes, and the auxiliary equipment is given elsewhere^[5]. The electrodes were 15 mm duraluminum plates and glass plates coated with a conducting layer of SnO_2 with a resistivity of 100 ohm-cm and a transmission of 85%, which permitted photographing the tracks through the electrode.

Each chamber was evacuated by a fore pump to a vacuum of ~ 0.1 mm Hg, and filled with an inert gas (Ne, Ar, He, Xe, and their mixtures) to a pressure $p \leq 1$ atm. The chamber was controlled by a Geiger counter telescope which selected cosmic ray particles passing through the chamber volume. A block diagram of the arrangement is shown in Fig. 1. A pulse from the coincidence circuit triggered the pulse generator at the TGI-1-325/16 hydrogen thyatron, whose pulse of ~ 16 kV height fired the first spark gap of the high

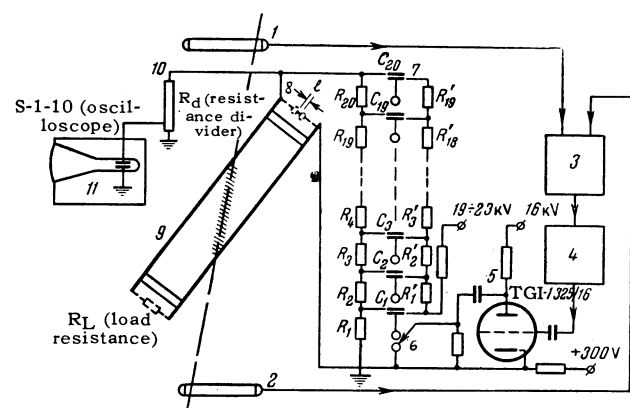


FIG. 1. Block diagram of the apparatus: 1, 2) rows of Geiger counters; 3) coincidence circuit; 4) amplifier and discriminator circuit; 5) pulser; 6) first spark gap of the HVPG; 7) HVPG; 8) shunting spark gap; 9) chamber; 10) high voltage divider; 11) oscilloscope.

voltage pulse generator (HVPG). The HVPG was a 20-stage unit of the Arkad'ev-Marx type^[14] using type 9KV10 capacitors ($C = 0.01 \mu\text{F}$, $V_{\text{max}} = 23$ kV). The maximum nominal pulse amplitude of the HVPG was 460 kV. The output voltage pulse could be taken from any stage of the HVPG, which permitted changing the pulse amplitude on the chamber in steps of $\Delta V = 19-23$ kV. The electronic delay in the application of the high voltage pulse relative to the Geiger counter pulse was $0.6 \mu\text{sec}$. The chamber capacity was $C_K \approx 50$ pF for the chamber with $d = 10$ cm and $C_K \approx 20$ pF for the chamber with $d = 25$ cm.

The high voltage pulse from the HVPG was observed with a type S-1-10 oscilloscope by means of a high voltage divider of pure resistances. The typical pulse shape is shown in Fig. 2. The pulse had a rise time $\tau_r \approx 15-20$ nsec, determined by the inductance and capacitance of the HVPG discharge circuit, which depend on the number of stages connected, and an exponential fall with a time constant $t_c \approx (C_{\text{out}} + C_K)R_L$, where $C_{\text{out}} = C/m$ is the output capacitance of the HVPG, $C = 0.01 \mu\text{F}$ is the capacitance of one stage of the HVPG, m is the number of stages connected, R_L is the load resistance connected in parallel with the chamber. To shape a high voltage pulse of length $\tau \approx 20-50$ nsec, a shunting air spark gap was used which consisted of two nickel-plated spheres 20 mm in diameter, fastened directly to the chamber electrodes. The pulse shape obtained with the shunting spark gap is shown by the solid line in Fig. 2. The pulse length τ represents the delay time in breakdown of the shunting gap, and the fall time is determined by the time of commutation (development of the spark channel) of the shunting gap and amounted in our case to $7-10$ nsec. The times τ and τ_f depend on the operating conditions of the shunting gap: the shape and height of the HVPG pulse (τ_r , overvoltage), the pressure and type of gas, and the intensity of illumination of the spark gap by ultraviolet light^[15]. In the shunting gap used, τ was changed by changing the distance between the electrodes of the gap. This type of control of the high voltage pulse length is simple and, as it turned out, adequate for stable oper-

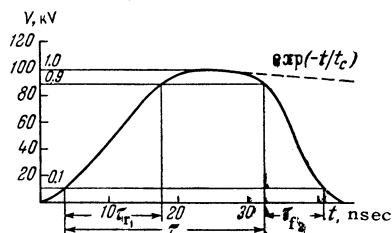


FIG. 2. High voltage pulse shape.

ation. For example, in the chamber with 10 cm electrode spacing, for pulse heights of 60–100 kV the distance between the shunting gap electrodes was 15–18 mm. Changing this distance by 1.5–2 mm led in every case to a change in track width in the chamber (the length of the streamer column) from 0 to several centimeters.

The particle tracks were photographed with two lenses: through the side wall (perpendicular to the electric field E) by an R-Biotar objective (aperture $f/0.85$) and through the transparent glass electrode (along the direction of E) by a Jupiter-3 objective ($f/1.5$). The photography was done with type 13 film (sensitivity 3000 GOST units).

MECHANISM OF OPERATION OF A STREAMER CHAMBER

In order to understand the operation of the chamber described, let us consider the streamer mechanism of development of a spark breakdown between two plane electrodes. Figure 3 shows schematically the stages of the gas discharge, from the initial acceleration of one of the primary electrons created by a particle in the chamber gas, to the establishment of a spark^[16]. An electron (a), accelerated in the electric field E , creates an electron shower (b) which, advancing toward the anode with a velocity of the order of 10^7 cm/sec ($E/p \approx 15$ V/cm · mm Hg), ionizes and excites in its path a continuous succession of new gas molecules. As the shower (b) grows, a larger and larger role is played by the space charge created by it and by the excited atomic states. The space charge, negative in the head of the shower (electrons) and positive in its tail (ions), creates its own field E_R , which distorts the external field (d). Photons from excited atoms with excitation energy higher than the ionization potential produce photoelectrons in the gas (e), which immediately move under the influence of the field $E + E_R$, and create

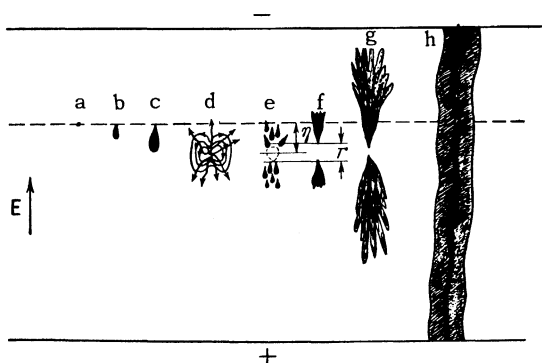


FIG. 3. Drawing of the streamer mechanism of the development of a spark breakdown in a spark chamber.

secondary showers which are added to the cloud of positive space charge. The combined action of the space charge and the photoionization in the gas volume leads to the result that, beginning at a certain time, the shower transfers to a streamer, which is a column of neutral plasma (f). The transition of a shower to a streamer occurs at the place where the field E_R is of the same order of magnitude as the field E , and the ionization density reaches a critical value (the so-called condition of Meek and Loeb^[16]). From this place, two streamer columns begin to grow, propagating in opposite directions with a velocity of $\sim 10^8$ cm/sec.

In travelling toward the electrode the streamer breaks up into many fine branches and has the form of a brush (g) (see also Fig. 4a). After the space between the electrodes is filled by streamers, current from the external circuit flows along the plasma column just as along a wire, which still further ionizes the gas and creates the spark channel (h) observed in a spark chamber. The track in a projection spark chamber consists of a number of such sparks formed along the particle path.

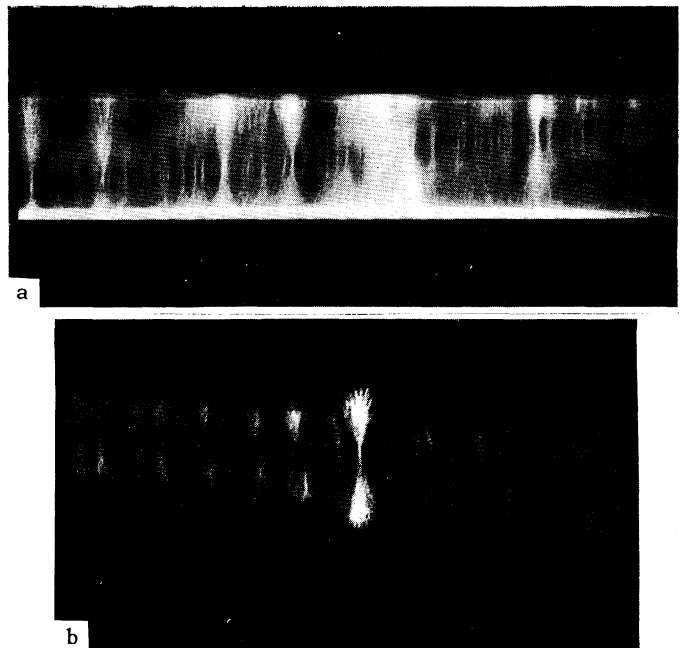


FIG. 4. Photographs of particle tracks in a streamer chamber filled with neon, taken through the side wall. $E = 8$ kV/cm.

In a streamer chamber, because a high voltage pulse of short duration ($\tau \approx 20$ – 50 nsec) is used, the discharge does not grow to the spark stage, but is cut off at the streamer stage (f or g). The particle track in a streamer chamber is formed by a number of streamers which have developed along the path, and which indicate the place of passage of the particle not only in projection on the elec-

trode but also along the coordinate parallel to the field \mathbf{E} (the coordinate z). The luminescence of the gas in the streamer channels makes the track visible, but the brightness of the streamer luminescence, which is proportional to the quantity of ionized gas, is much less than the brightness of the sparks in spark chambers.

PARTICLE TRACKS IN A STREAMER CHAMBER

Figure 4 shows photographs of particle tracks observed through the side wall of a streamer chamber filled with neon to a pressure $p \approx 1$ atm, obtained by successive reduction of the pulse length τ . Whereas for a pulse length $\gtrsim 200$ nsec there is formed along the particle path a solid wall of sparks which mask the place of passage of the particle, on the other hand for $\tau \approx 100$ nsec the discharge does not develop beyond the stage of long streamers and the particle track is clearly distinguished in its z coordinate (Fig. 4a). Further reduction in pulse length results in the recording of only the initial parts of the streamers, and the particle track width δ , determined by the distance travelled by the streamers, is reduced. The particle track width shown in Fig. 4b is ~ 12 mm for a pulse length $\tau \approx 35$ nsec. With further narrowing of the tracks, their brightness is sharply decreased, so that for $\delta = 7$ mm they are not recorded on photographic film, although they



FIG. 5. Photograph of a particle track in a neon-filled streamer chamber ($p = 1$ atm, $E = 8$ kV/cm), obtained with a long rise time of the high voltage pulse.

are observed visually quite well down to $\delta \approx 2$ mm.

As can be seen from Fig. 4b, a particle track in a streamer chamber consists of bright strips, parts of streamers, whose length and brightness vary because of fluctuations in the development of individual electron showers and streamers. The strips have characteristic constrictions in the middle which indicate the place of origin of the streamers (the region r , Fig. 3f), and the wide parts on either side of the constriction are the positive and negative streamers, growing in opposite directions.

The "fine structure" of the particle track is especially distinct in Fig. 5. Here is shown a photograph of a single particle in a streamer chamber, taken with a resistance of ~ 1 k Ω connected in series with the chamber, which increases the rise time of the pulse to $\tau_r \approx 50$ –100 nsec. The constrictions are converted into a dark band, dividing the track in half, in which are located the initial parts of the streamers with a brightness below the threshold sensitivity of the photographic film (and of the eye).

The z -coordinates of the particle path, which are located in the middle of the track (at the constrictions), are determined with an accuracy of 1 mm. These points are shifted relative to the true path by the distance η travelled by the shower up to its transfer to a streamer (Fig. 3e). η is determined by the parameters of the high voltage pulse and in our case $\eta \approx 1$ mm. The stability of operation of the shunting spark gap, which determines the stability of the pulse length τ and the fall time τ_f , is such that the time spread $\Delta\tau \approx 1$ nsec, which leads to a spread in track width $\Delta\delta/\delta \approx 25\%$ for $\delta \approx 10$ mm.

Particle tracks in a streamer chamber are noticeably brighter when projected on the transparent electrode, since each streamer is projected to a dot of size $\lesssim 1$ mm. Figure 6 shows photographs of particle tracks in this projection. A particle track consists of successive bright spots whose density along the track is ~ 2 per cm, and of diffuse illumination between the spots. Figure 6a shows the track of a single particle. The two bright spots somewhat off the track apparently are δ -ray tracks. Figure 6b shows a pair of particles moving apart at a small angle.

Particle tracks in a streamer chamber, photographed along the electric field, are more uniform in brightness and width than in a projection spark chamber^[5], the spread of the spots relative to the median line is less, and consequently the accuracy of localization is greater.

Figure 7 shows a photograph of three particles

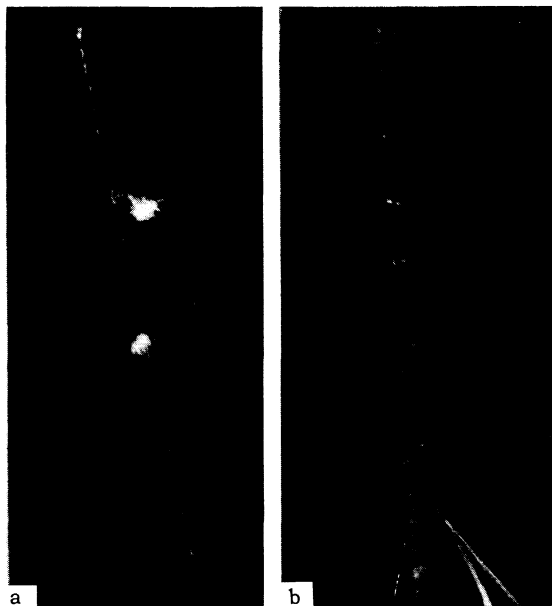


FIG. 6. Photographs of particle tracks in a streamer chamber obtained by photographing through the transparent electrode.

passing simultaneously through a streamer chamber filled with neon ($p = 1$ atm). Although the question of the simultaneous recording of many particles in a streamer chamber requires further experimental study, we can say a priori that the currents flowing in the circuit of a streamer chamber at the time when the particles are recorded are substantially less than the corresponding currents in a spark chamber. Therefore particle tracks are formed considerably more independently of each other in a streamer chamber than in a spark chamber, and the recording of a large number, apparently, should not encounter any difficulties.

We can see from Fig. 7 that the brightness and nature of the tracks depend on the angle φ between the particle trajectory and the direction of the electric field \mathbf{E} . The track brightness is least for $\varphi \approx 90^\circ$ and gradually increases with decrease of φ . At the same time the track structure also changes from a discontinuous series of separate streamers, for $\varphi \approx 60-90^\circ$, to a solid plasma filament for $\varphi < 60^\circ$; with a decrease of φ the filament becomes thinner and brighter. Thus a streamer chamber, while distinguished from a spark chamber by its isotropy of recording efficiency and degree of localization of particles, has an anisotropy in the brightness and structure of the tracks. The variation in track brightness is an important deficiency of the streamer chamber, which complicates, in particular, the photography, and also the possibility of measuring primary ionization.



FIG. 7. Photograph of a shower of three particles.

INVESTIGATION OF DIFFERENT GAS FILLINGS

The chamber was filled with the noble gases He, Ne, Ar, Xe, and mixtures of Ne + Ar, Ne + Xe, and He + Xe in different proportions. The pressure was varied from 100 to 760 mm Hg. The nature of the tracks was the same in all cases, but the track brightness was appreciably different. With visual observation the best track brightness was obtained in Ne; the other gases give tracks of lower brightness. Addition to Ne of admixtures of Ar or Xe (up to 10%) did not increase the track brightness. Apparently this is due to the fact that the increase in ionization coefficient in such mixtures, connected with collisions of the second kind, is unimportant in this case because of the short duration of the high voltage pulse.

Use of spectroscopically pure Ne also did not increase the track brightness. This question was investigated by observation of particle tracks in a 2-liter sealed glass bulb filled with spectroscopically pure Ne.

We investigated the chamber operation with Ne for a variation of the gas pressure from 50 to 760 mm Hg, with the aim of observing the variation of streamer column density with primary ionization. In these measurements the parameters of the high voltage pulse were chosen to keep the track width about the same at the different pressures. We found that in the pressure interval 300–760 mm Hg the streamer density is practically constant (~ 2 per cm). At lower pressures the observed streamer density decreases monotonically, which is evidently due to the decrease in primary ionization. The absence of an increase in streamer

density with pressure above 300 mm Hg may result from fluctuations in the time of electron shower development and in the suppression, which is related to this mechanism, of a retarded streamer by the space charge field of a neighboring streamer.

CONCLUSION

The gas-discharge track detector described—the streamer chamber—is a fast acting apparatus with isotropic efficiency for recording and localizing particles, and also the possibility of recording spatial events. However, the brightness and structure of the track depend on the direction of the particle trajectory with respect to the electric field in the chamber. Furthermore, particle tracks in the chamber are not very bright and are rather wide in the electric field direction (7–10 mm), which impairs the spatial resolution. In the future it may be possible to remove these deficiencies by improving the parameters of the electrical pulse.

At the same time, the advantages of the streamer chamber over the spark chamber are already evident in such important parameters as dead time (since the ionization density in the volume of a streamer chamber is substantially less) and the possibility of measuring the ionizing ability of particles. As a measure of ionizing ability we can utilize the density of streamer columns, their size, and their brightness.

In conclusion we wish to note that the streamer chamber is a very interesting tool for the study of processes related to the physics of a gas discharge. Streamer velocity, electron shower path length, fluctuation processes in showers, and many other characteristics of a discharge can be successfully studied with apparatus of this type, where the primary electrons which initiate the discharge are accurately localized in the region between the electrodes.

The authors thank Professor A. I. Alikhanyan for his interest in this work; Yu. Grashin, S. Somov, V. Chizhov, and V. Dmitrenko of the research laboratory of the Moscow Engineering Physics Institute, L. V. Sukhov of the Physics Institute of the Academy of Sciences for major help in the investigation, and V. Rykalin of the Laboratory for Nuclear Problems of the Joint Institute for Nuclear Research for kindly supplying the photographic film.

¹B. A. Dolgoshein and B. I. Luchkov, JETP 46, 392 (1964), Soviet Physics JETP 19, 266 (1964). Mikhaïlov, Roinishvili, and Chikovani, JETP 45, 818 (1963), Soviet Phys. JETP 18, 561 (1964); JETP 46, 1228 (1964), Soviet Phys. JETP 19, 833 (1964).

²M. I. Daïon and G. A. Leksin, UFN 80, 281 (1963), Soviet Phys. Uspekhi 6, 428 (1963).

³Proc. of the 1962 Conf. on Instr. for High Energy Physics, CERN, Geneva, 1963. Nucl. Instr. Meth. 20, 143 (1963).

⁴Cronin, Engels, Pyka, and Roth, Rev. Sci. Instr. 33, 946 (1962).

⁵Dolgoshein, Luchkov, and Moiseev, PTÉ (in press).

⁶M. I. Daïon, Voprosy fiziki elementarnykh chastits (Problems of Elementary Particle Physics), AN ArmSSR, Erevan, 1963.

⁷A. I. Alikhanyan, Voprosy fiziki elementarnykh chastits (Problems of Elementary Particle Physics), AN ArmSSR, Erevan, 1963.

⁸Bolotov, Daïon, Devishev, Klimanova, Luchkov, and Shmeleva, PTE, No. 2, 57 (1964).

⁹Alikhanyan, Asatiani, and Matevosyan, JETP 44, 773 (1963), Soviet Phys. JETP 17, 522 (1963).

¹⁰V. N. Bolotov and M. I. Devishev, Nucl. Instr. Meth. (in press).

¹¹S. Fukui and B. Zacharov, Nucl. Instr. Instr. Meth. 23, 24 (1963).

¹²Fukui, Hayakawa, Tsukishima, and Nukushina, Nucl. Instr. Meth. 20, 236 (1963).

¹³Cavalleri, Gatti, and Redaelli, Nuovo cimento 25, 1282 (1962).

¹⁴Vysokovol'tnoe ispytatel'noe oborudovanie i izmereniya (High Voltage Apparatus and Measurements), edited by A. A. Vorob'ev, Gostekhizdat, 1960.

¹⁵G. A. Mesyats, dissertation, Tomsk University, 1961.

¹⁶J. M. Meek and J. D. Craigs, Electrical Breakdown of Gases, Oxford, Clarendon Press, 1953 (Russ. Transl., IIL, 1956).

Translated by C. S. Robinson